EPJ Web of Conferences **171**, 04004 (2018) https://doi.org/10.1051/epjconf/201817104004
SQM 2017

Update on Heavy Flavor Production in Cold Matter

R. Vogt[1,2,a]

[1]*Nuclear and Chemical Sciences Division, Lawrence Livermore National Laboratory, Livermore, CA 94550, USA*
[2]*Physics Department, University of California at Davis, Davis, CA 95616, USA*

Abstract. I will discuss areas of heavy flavor theory where new progress has been made.

1 Introduction

I first focus on open heavy flavor and quarkonium production in $p + p$ collisions before going on to discuss some effects due to cold nuclear matter. The length of a conference proceeding is too short for a complete review of these topics in $p + p$ and $p + A$ interactions. For a somewhat more detailed discussion of open heavy flavor and quarkonium production in $p + p$ collisions, as well as additional references, see Ref. [1].

2 Open heavy flavor production

There are currently two approaches to heavy flavor production at colliders: collinear factorization and low x k_T-factorization approach. I briefly describe each one as applied to single inclusive heavy flavor observables. I then turn to exclusive observables and correlated heavy quark pair production.

There are two main methods of calculating the spectrum of single inclusive open heavy flavor production in perturbative QCD assuming collinear factorization. The underlying idea is similar but the technical approach differs. Both note that large logarithms of p_T/m arise at all orders of the perturbative expansion, spoiling the convergence. The first terms in the expansion are the leading (LL) and next-to-leading logarithmic (NLL) terms, $\alpha_s^2[\alpha_s \log(p_T/m)]^k$ and $\alpha_s^3[\alpha_s \log(p_T/m)]^k$ respectively.

It is worth noting that the single inclusive heavy flavor p_T distribution is finite at leading order (LO) as $p_T \to 0$ because of the finite quark mass scale. A next-to-leading order (NLO) calculation that assumes production of massive quarks but neglects LL terms, a "massive" formalism, can result in large uncertainties at high p_T [2–4]. (This massive formalism is sometimes referred to as a fixed-flavor-number (FFN) scheme.) If, instead, the heavy quark is treated as "massless" and the LL and NLL corrections absorbed into the fragmentation functions, the approach breaks down as p_T approaches m even though it improves the result at high p_T. The massless formalism is also sometimes referred to as the zero-mass, variable-flavor-number (ZM-VFN) scheme [5, 6]. There are schemes which interpolate smoothly between the FO/FFN scheme at low p_T and the massless/ZM-VFN scheme. The fixed-order next-to-leading logarithm (FONLL) approach is one such scheme. In

[a]e-mail: rlvogt@lbl.gov

FONLL, the fixed order and fragmentation function approaches are merged so that the mass effects are included in an exact calculation of the leading (α_s^2) and next-to-leading (α_s^3) order cross section while also including the LL and NLL terms [7]. The NLO fixed order (FO) result is combined with a calculation of the resumed (RS) cross section in the massless limit. The FO and RS approaches need to be calculated in the same renormalization scheme. The FONLL result is then, schematically,

$$\text{FONLL} = \text{FO} + (\text{RS} - \text{FOM0})G(m, p_T) \; . \tag{1}$$

The interpolating function $G(m, p_T) \sim p_T^2/(p_T^2 + (cm)^2)$ is arbitrary but must approach unity for $m/p_T \to 0$. Fragmentation functions for D and D^* mesons have been calculated in an approach consistent with an FONLL calculation [8]. The second interpolation scheme is the generalized-mass variable-flavor-number (GM-VFN) scheme [9]. The large logarithms in charm production for $p_T \gg m$ are absorbed in the charm parton distribution function and can thus be evolved by the evolution equations for the parton distributions. The logarithmic terms can be incorporated into the hard cross section to achieve better accuracy for $p_T \geq m$. By adjusting the mass-dependent subtraction terms, no interpolating function is required [9].

In the k_T-factorization approach, off-shell leading order matrix elements for $g^*g^* \to c\bar{c}$ are used together with unintegrated gluon densities that depend on the transverse momentum of the gluon, k_T, as well as the usual dependence on x and μ_F. The motivation for choosing the k_T-factorized approach is that, at sufficiently low x, collinear factorization should no longer hold.

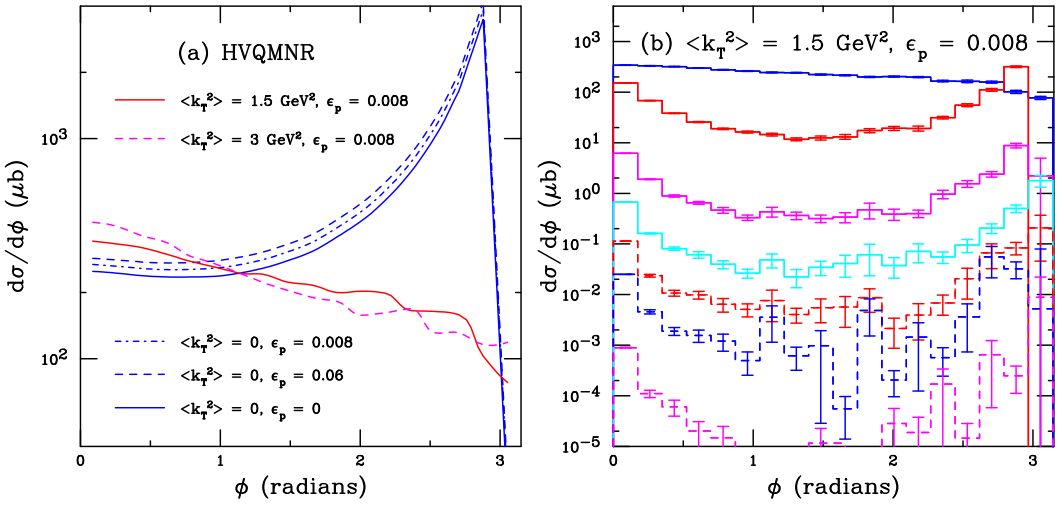

Figure 1. Calculations of the NLO azimuthal distribution between two charm quarks using the HVQMNR code at $\sqrt{s}$ = 7 TeV and forward rapidity. (a) The blue solid, dashed and dot-dashed curves, all without k_T broadening, show the effect of modifying the charm fragmentation function. The red solid curve uses a k_T broadening consistent with J/ψ production at 7 TeV [14] while the dashed magenta curve shows the effect of doubling the k_T broadening. (b) Using $\langle k_T^2 \rangle$ = 1.5 GeV^2 and ϵ_p = 0.008 from the solid red curve in (a), the p_T cuts on the charm quarks are varied. From top to bottom the results are: p_T < 10 GeV; p_T > 10 GeV; p_T > 20 GeV; p_T > 30 GeV; p_T > 40 GeV; p_T > 50 GeV; p_T > 75 GeV. The curves for all but the lowest p_T cut are scaled up by 10^3.

The LHC data has been compared to calculations in both approaches and those assuming collinear factorization compare well with the LHC data. Recent ALICE data [10], at $0 < p_T < 2$ GeV supports

collinear factorization. Their D^0 results at 7 TeV for $|y| < 0.5$, were compared to FONLL, GV-VFNS and LO k_T-factorization calculations. Only the k_T-factorized calculation is inconsistent with the shape of the data in the p_T range where the calculation should best apply. The forward rapidity data of LHCb at 7 TeV [11] and 13 TeV [12], also agree well with the collinear factorization assumption. The recent 13 TeV data from LHCb is within the uncertainty bands of FONLL and POWHEG (discussed below) down to $p_T \to 0$, albeit with large uncertainty bands and near the upper limit of the band. The GM-VFNS calculation is given only for $p_T > 3$ GeV but agrees well with the data with small uncertainties [12]. Perhaps a NLO k_T-factorized result could lead to improved agreement with the data but so far collinear factorization appears to still work well for low x charm production.

A further challenge to theory may arise from measurements of correlated production, specifically of the azimuthal opening angle of heavy flavors, either by direct reconstruction of both D mesons or of a D meson and the decay product of its partner, either a light hadron or a lepton [13]. Naively, at LO $Q\overline{Q}$ pairs are produced back-to-back with a peak at $\Delta\phi = \pi$. Higher order production will, however, result in a more isotropic distribution in $\Delta\phi$ due to light parton emission in the final state.

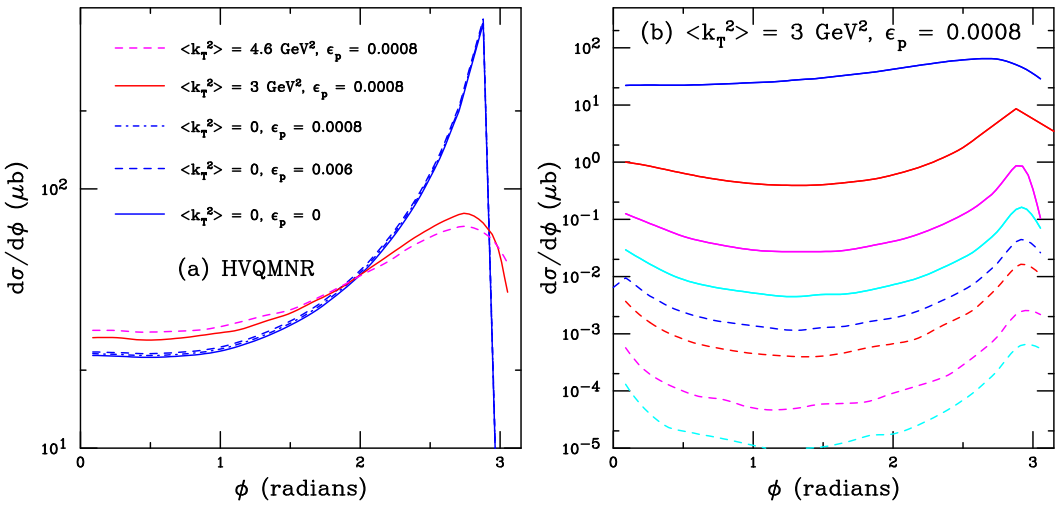

Figure 2. Calculations of the NLO azimuthal distribution between two bottom quarks using the HVQMNR code at $\sqrt{s} = 7$ TeV and forward midrapidity. (a) The blue solid, dashed and dot-dashed curves, all without k_T broadening, show the effect of modifying the charm fragmentation function. The red solid curve uses the k_T broadening for Υ production at 7 TeV while the dashed magenta curve shows the effect of doubling the k_T broadening. (b) Using $\langle k_T^2 \rangle = 3$ GeV^2 and $\epsilon_p = 0.0008$ from the solid red curve in (a), the p_T cuts on the bottom quarks are varied. From top to bottom the results are: $p_T < 10$ GeV; $p_T > 10$ GeV; $p_T > 20$ GeV; $p_T > 30$ GeV; $p_T > 40$ GeV; $p_T > 50$ GeV; $p_T > 75$ GeV and $p_T > 100$ GeV. No scale factor is included on the results.

The FONLL and GM-VFNS approaches are for single inclusive production only. There are NLO heavy flavor codes that, in addition to inclusive heavy flavor production, also calculate exclusive $Q\overline{Q}$ pair production. HVQMNR [15] uses negative weight events used to cancel divergences numerically. Smearing the parton momentum through the introduction of intrinsic transverse momenta, k_T, reduces the importance of the negative weight events. HVQMNR does not include any resummation. POWHEG – hvq [16] is a positive weight generator that includes leading-log resummation. The entire event is available since PYTHIA [17] and HERWIG [18] are employed to produce the complete event. In addition to these NLO codes, heavy flavor correlations can also be simulated employing LO event

generators such as PYTHIA. The k_T-factorization approach can also be employed to calculate correlated $c\overline{c}$ production since the unintegrated parton densities have a transverse component, giving finite p_T and $\Delta\phi$ distributions even at LO.

There are LHC data, particularly from ALICE [19] and LHCb [20], on charm pair correlations to test these approaches.

LHCb measured $c\overline{c}$, cc, and cJ/ψ correlations in $p + p$ collisions at 7 TeV for $2 < y < 4$. About 10% of the $c\overline{c}$ rate was found in the cc and cJ/ψ channels [20]. Only the $c\overline{c}$ pairs can be produced in a single hard scattering. The other events are more consistent with production through double parton scattering. The azimuthal and rapidity distributions for the cc events are consistent with isotropic emission [20], as might be expected from two hard scatterings.

The ALICE collaboration recently presented an analysis of azimuthal correlations between reconstructed D mesons and a light hadron trigger particle [19]. The light hadrons were primary particles, emitted from the collision points. These particles include those from heavy flavor decays, such as the unreconstructed partner D meson. The data were binned according to the transverse momentum of both the D meson and the light hadron. The minimum light hadron p_T was soft, $p_T > 0.3$ GeV. These data were further subdivided into two p_T ranges, $0.3 < p_T < 1$ GeV and $p_T > 1$ GeV. The D meson p_T was considerably higher: $3 < p_T < 5$ GeV, $5 < p_T < 8$ GeV, and $8 < p_T < 16$ GeV. To improve statistics, the "D meson" is an average over the D^0, D^+ and $D*^+$. The ALICE measurements cover the central region, $|y| < 0.5$ for the D and $|\Delta\eta| < 1$ for the light hadron. The general behavior is, however, the same as the LHCb $D^0\overline{D}^0$ pairs, a peak at $\Delta\phi = 0$ and a smaller enhancement at $\Delta\phi = \pi$. The peak at $\Delta\phi = 0$ increases with increasing trigger particle p_T and also with increasing D meson p_T. The data were compared to simulations with various PYTHIA tunes and also POWHEG+PYTHIA. All simulations reproduced the trends of the data [19].

Figure 1(a) shows how the ϕ distribution between the c and $\overline{c}$ changes with the fragmentation parameter ϵ_p and the strength of the k_T broadening chosen. Note that the NLO result is not a delta function at $\phi = \pi$, as at LO, due to the emission of light partons in the final state, even when $\epsilon_p = 0$. Changing ϵ_p does not have a strong effect on the shape of $d\sigma/d\phi$. However, introducing k_T broadening changes $d\sigma/d\phi$ from peaked at $\phi \sim \pi$ to more isotropic with a maximum at $\phi = 0$ instead. No p_T cut is made on the momentum of the charm quarks. The effect of a p_T-dependent cut on the charm quarks is explored in Fig. 1(b) using $\langle k_T^2 \rangle = 1.5$ GeV^2, consistent with the broadening needed to describe the J/ψ p_T dependence in Ref. [14], and $\epsilon_p = 0.008$, softer than the traditional Peterson function. With these choices, the HVQMNR p_T distribution is in agreement with the FONLL D^0 p_T distribution for the same choice of charm mass and scale parameters. When only low p_T charm quarks are considered, $p_T < 10$ GeV, the azimuthal distribution is rather flat. Increasing the p_T cut on the charm quarks results in distributions that are peaked at $\phi = 0$ and π: either the charm quarks are aligned opposite a high momentum light parton ($\phi = 0$) or the charm quarks are effectively back-to-back with a soft light parton emitted ($\phi \sim \pi$).

Figure 2 shows a similar calculation for bottom quarks. The effect of changing the fragmentation function is reduced for the heavier bottom quarks, as is the effect of k_T broadening. The harder p_T dependence for b quarks allows the azimuthal distribution to be calculated at higher p_T, up to $p_T > 100$ GeV with higher statistics. The same trends are observed for bottom and charm quarks.

It appears that, so far, the open charm results presented by the LHC collaborations, both single inclusive production and charm pair correlations, are in agreement with calculations based on collinear factorization with single hard scatterings. The exception, the cc and cJ/ψ events at LHCb, are consistent with double parton scattering.

3 Quarkonium Production

I now turn to quarkonium production. Perturbative QCD is employed to calculate the production characteristics. A number of models have been used since the discovery of the J/ψ just over 40 years ago. One of the first was the color evaporation model (CEM) [21–23] which does not specify the color or spin state of the produced $Q\overline{Q}$ pairs. The next was the color singlet model (CSM) [24] which only considered quarkonium states produced as color neutral objects. Despite the addition of a number of higher order corrections, a good description of the data has not been achieved. The current most successful approach, non-relativistic QCD (NRQCD) [25, 26], is based on an expansion of the cross section in both the strong coupling constant and $Q\overline{Q}$ velocity with a separation of the hard and soft scales so that contributions to the cross section are divided into different color states with different weight factors, long distance matrix elements (LDMEs), assumed to be universal, which are adjusted to data. Most calculations have been done in the collinear factorization approach. However, some work has also been done in k_T-factorization both in the context of the CSM and NRQCD. In the remainder of this section, I will discuss only recent results in NRQCD and the CEM.

According to the NRQCD factorization theorem for J/ψ production, the production cross section can be written as

$$\sigma_{J/\psi} = \Sigma_n \sigma_{c\overline{c}[n]} \langle \mathcal{O}^{J/\psi}[n] \rangle \tag{2}$$

where the sum over n includes all Fock states, including color octet states [25]. The cross section $\sigma_{c\overline{c}[n]}$ is the production rate of a $c\overline{c}$ pair in the color and spin state n, calculated in perturbative QCD. Finally, $\langle \mathcal{O}^{J/\psi}[n] \rangle$ represents the LDMEs which describe the conversion of the $c\overline{c}[n]$ state into a final state J/ψ, assuming that the hadronization does not change the spin or momentum. The full cross section includes convolution with the parton densities appropriate to the process in question.

In comparisons of the NRQCD calculations to data, the color octet LDMEs are determined above some p_T cut, along with uncertainty on their values. The uncertainty band is determined by fixing the LDMEs to their central fit values and varying the renormalization and factorization scales by a factor of two relative to the central values of $\mu_R = \mu_F = m_T = (p_T^2 + 4m_c^2)^{1/2}$ with $m_c = 1.5$ GeV. No variation of the charm quark mass or the LDMEs are included in the uncertainty band [26].

One of the most important questions for NRQCD to resolve is whether or not the color octet LDMEs are indeed universal. Their universality has been called into increasing question recently. Different groups arrive at different values of the LDMEs depending on the chosen p_T cut, the data sets included in the analysis, and whether or not the polarization data are included in the fits, see Ref. [26] and references therein. In addition, the LDMEs fit to collider data do not agree with the integrated cross sections, $d\sigma/dy|_{y=0}$ [27]. Recent measurements of the η_c at forward rapidity in LHCb [28] strongly disagree with the p_T distributions calculated assuming heavy quark spin symmetry [29].

If one goes beyond current next-to-leading order (NLO) calculations, it is not clear that the p_T dependence would substantially change. The p_T distributions already include the powers giving the hardest p_T distributions. Adopting more fit parameters, including the mass and scales, will not have a strong effect on the p_T distributions. Changing the factorization scale has the largest effect on the shape but modifying the renormalization scale or the quark mass has a larger effect on the magnitude than the shape of the distributions.

It has been suggested that NRQCD factorization does not hold for polarization. However, if factorization holds for the p_T distributions, then, under the assumption that the spin and momentum are unaffected by hadronization, the initial polarization should survive as well.

The difficulties that have plagued the NRQCD description of J/ψ production are reduced for Υ production. The larger mass, higher scale and lower velocity could make the Υ a better candidate for an accurate description by NRQCD. In addition, since there are more Υ states, there are more

color octet LDMEs available for fitting, allowing a description of the p_T-dependent yields and the polarization simultaneously.

Some new developments to the color evaporation model make it worth a second look. In the CEM, heavy flavor and quarkonium production is treated on an equal footing. In the CEM, the quarkonium production cross section is some fraction of all $Q\overline{Q}$ pairs below the $H\overline{H}$ threshold where H is the lowest mass heavy-flavor hadron. Thus the CEM cross section is simply the $Q\overline{Q}$ production cross section with a cut on the pair mass. The color and spin have been integrated over so that the color of the state is said to have been 'evaporated' away without changing the kinematics of the pair.

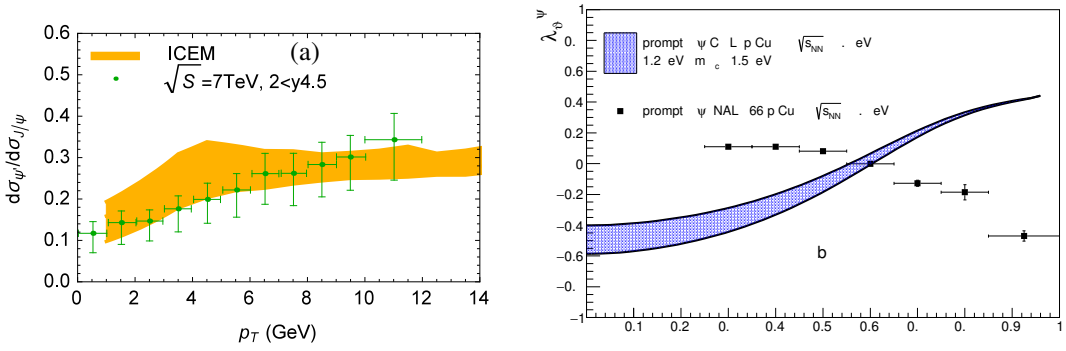

Figure 3. (a) Results for ratio of the ψ' to J/ψ production cross sections at forward rapidity for 7 TeV $p + p$ collisions [30]. (b) The x_F dependence of the polarization parameter λ_θ for prompt production of J/ψ in p+Cu collisions at $\sqrt{s_{NN}}$ = 38.8 GeV is compared to the E866/NuSea data. The horizontal uncertainties are the experimental bin widths. From [31].

At leading order, the production cross section of quarkonium state C in a $p + p$ collision is

$$\sigma_C^{\rm CEM}(s_{NN}) = F_C \sum_{i,j} \int_{M^2}^{4m_H^2} d\hat{s} \int dx_1\, dx_2\, f_i^p(x_1,\mu_F^2)\, f_j^p(x_2,\mu_F^2)\, \mathcal{J}(\hat{s})\hat{\sigma}_{ij}(\hat{s},\mu_F^2,\mu_R^2)\ , \tag{3}$$

where $ij = q\overline{q}$ or gg and $\hat{\sigma}_{ij}(\hat{s})$ is the $ij \to Q\overline{Q}$ subprocess cross section. Here $\mathcal{J}(\hat{s})$ is a kinematics-dependent Jacobian. In the traditional CEM, the lower limit on the integration over $\hat{s}$ is $M^2 = 4m_c^2$. The fraction F_C must be universal so that, once it is fixed by data, the quarkonium production ratios should be constant as a function of $\sqrt{s}$, y and p_T. The actual value of F_C depends on the heavy quark mass, m, the scale parameters, the parton densities and the order of the calculation. The same values of the charm quark mass and scale parameters as found in Ref. [14] are employed to obtain the normalization F_C for the J/ψ,

Two recent updates of the CEM are worth noting. The first is a calculation of the ψ'/ψ ratio as a function of p_T in an "improved" CEM calculation (ICEM) [30]. In this calculation, the p_T of the quarkonium state is modified by the ratio of the pair invariant mass to the quarkonium mass, M_C. In addition, the lower limit on the integral is now $M^2 = M_C^2$. Thus a rise in the ratio with p_T consistent with measurement is found [30], see Fig. 3(a). The second is the first calculation of polarization in the CEM. If one assumes that the spin of the quarks are either aligned or anti-aligned with the momentum, $J_z = -1, 0$ or 1, and this alignment, like the momentum of the quarks, survives hadronization, the polarization can be obtained. The first calculation separated the longitudinal and transverse components [32] while the second separated the S and P states to calculate the polarization parameter, λ_ψ

in the ICEM [31]. The results so far are at LO. Therefore, only comparison to fixed-order results is possible so far, as shown for p+Cu collisions at $\sqrt{s} = 38.8$ GeV. Work is underway to calculate the p_T dependence in the k_T-factorization approach before attempting a full NLO calculation.

4 Heavy Flavors in Cold Nuclear Matter

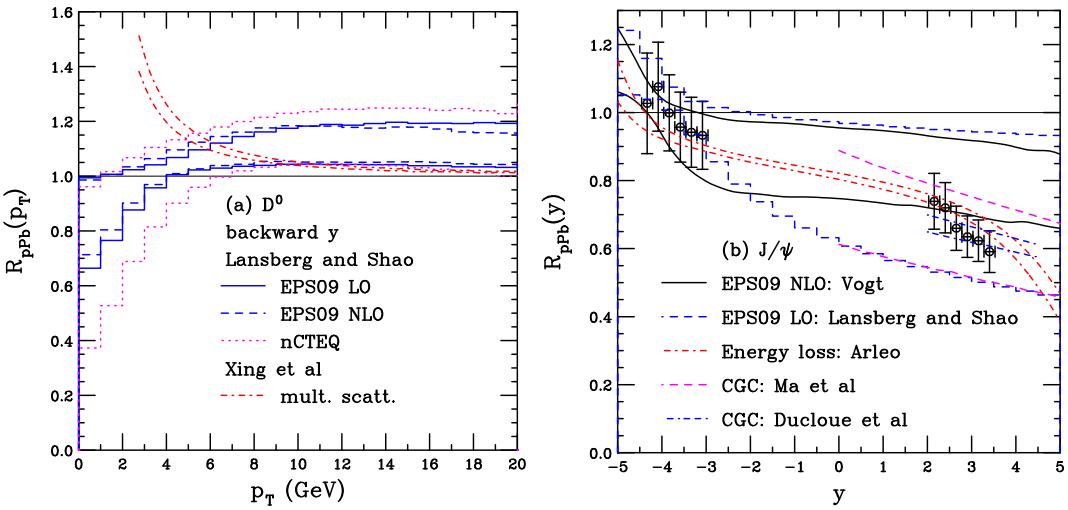

Figure 4. (a) The D^0-meson $R_{p\mathrm{Pb}}(p_T)$ at $-4 < y < -2.96$. The red band is by Xing *et al.*. The data-driven shadowing results of Lansberg and Shao at $-4.46 < y < -2.96$ are shown as histograms for EPS09 NLO (solid blue), EPS09 LO (dashed blue) and nCTEQ15 (dotted magenta). (b) The J/ψ $R_{p\mathrm{Pb}}(y)$ for EPS09 NLO by Vogt (black), the data-driven result from Lansberg and Shao for EPS09 LO (blue dashed histogram), the energy loss calculation by Arleo (dot-dashed red), and the CGC calculations by Doucloué *et al.* (blue dot-dashed) and Ma *et al.* (dashed magenta). The ALICE data [34] are shown in black. For details, see Albacete *et al.* [35].

There are several important cold nuclear matter (CNM) effects that need to be taken into account when determining the strength of deconfinement effects on a particular final state. These include modifications of the parton distribution functions in nuclei, either by shadowing in collinear factorization or through the color glass condensate (CGC) approach; energy loss and/or k_T broadening in the Cronin effect; and isospin effects, negligible for heavy flavor production. In addition, for quarkonium effects such as nuclear absorption and comover breakup may play a role. See Ref. [35] for a summary of these effects as well as predictions for the 8 TeV LHC p+Pb run and Refs. [33] for a summary for 5 TeV predictions as well as comparison to data.

Figure 4 shows results for (a) D^0 and (b) J/ψ modifications in p+Pb relative to $p+p$ collisions at 8 TeV. The multiple scattering model of D^0 modifications gives a significantly different ratio $R_{p\mathrm{Pb}}(p_T)$ at low p_T than the results with shadowing alone: one produces an enhancement while the other gives effective suppression. The J/ψ results as a function of rapidity are compared to preliminary ALICE data [34]. All the models give reasonable agreement with the data so far. Note that the CGC predictions are only shown at forward rapidity.

Acknowledgments

I thank the organizers for the invitation to give this talk. This work was performed under the auspices of the U.S. Department of Energy by Lawrence Livermore National Laboratory under Contract DE-AC52-07NA27344 and supported by the U.S. Department of Energy, Office of Science, Office of Nuclear Physics (Nuclear Theory) under contract number DE-SC-0004014.

References

[1] R. Vogt, EPJ Web Conf. **137** (2017) 01022.
[2] P. Nason *et al.*, Nucl. Phys. B **303** (1988) 607; B **327** (1988) 49; B **335** (1990) 260(E).
[3] W. Beenakker, H. Kuijf, W. L. van Neerven and J. Smith, Phys. Rev. D **40**, (1989) 54.
[4] W. Beenakker *et al.*, Nucl. Phys. B **351** (1991) 507.
[5] M. Cacciari and M. Greco, Nucl. Phys. B **421** (1994) 530.
[6] J. Binnewies, B. A. Kniehl and G. Kramer, Phys. Rev. D **58** (1998) 014014.
[7] M. Cacciari, M. Greco and P. Nason, JHEP **05** (1998) 007.
[8] M. Cacciari and P. Nason, JHEP **0309** (2003) 006.
[9] B. A. Kniehl, G. Kramer, I. Schienbein and H. Spiesberger, Phys. Rev. D **71** (2005) 014018.
[10] J. Adam *et al.* [ALICE Collaboration], Phys. Rev. C **94** (2016) 054908.
[11] R. Aaij *et al.* (LHCb Collaboration), Nucl. Phys. B **871** (2013) 1.
[12] R. Aaij *et al.* [LHCb Collaboration], JHEP **1603** (2016) 159, Erratum: [JHEP **1609** (2016) 013], Erratum: [JHEP **1705** (2017) 074]
[13] A. Mischke, Phys. Lett. B **671** (2009) 361.
[14] R. E. Nelson, R. Vogt and A. D. Frawley, Phys. Rev. C **87** (2013) 014908.
[15] M. L. Mangano, P. Nason, and G. Ridolfi, Nucl. Phys. B **373** (1992) 295.
[16] S. Frixione, P. Nason, and G. Ridolfi, JHEP **0709** (2007) 126; arXiv:0707.3081 [hep-ph].
[17] T. Sjostrand *et al.*, Comput. Phys. Commun. **135** (2001) 238; arXiv:hep-ph/0308153.
[18] G. Corcella *et al.*, JHEP **0101** (2001) 010.
[19] J. Adam *et al.* [ALICE Collaboration], Eur. Phys. J. C **77** (2017) 245.
[20] R. Aaij *et al.* [LHCb Collaboration], JHEP **1206** (2012) 141, [JHEP **1403** (2014) 108].
[21] R. Gavai *et al.*, Int. J. Mod. Phys. A **10** (1995) 3043.
[22] G. A. Schuler and R. Vogt, Phys. Lett. B **387** (1996) 181.
[23] J. F. Amundson, O. J. P. Eboli, E. M. Gregores and F. Halzen, Phys. Lett. B **390** (1997) 323.
[24] R. Baier and R. Rückl, Z. Phys. C **19** (1983) 251.
[25] G. T. Bodwin, E. Braaten and G. P. Lapage, Phys. Rev. D **51** (1995) 1125.
[26] N. Brambilla *et al.*, Eur. Phys. J. C **74** (2014) 2981.
[27] Y. Feng, J. P. Lansberg and J. X. Wang, Eur. Phys. J. C **75** (2015) 313.
[28] R. Aaij *et al.* [LHCb Collaboration], Eur. Phys. J. C **75** (2015) 311.
[29] M. Butenschön, Z.-G. He and B. A. Kniehl, Phys. Rev. Lett. **114** (2005) 092004.
[30] Y. Q. Ma and R. Vogt, Phys. Rev. D **94** (2016) 114029.
[31] V. Cheung and R. Vogt, Phys. Rev. D **96** (2017) 054014.
[32] V. Cheung and R. Vogt, Phys. Rev. D **95** (2017) 074021.
[33] J. L. Albacete *et al.*, Int. J. Mod. Phys. E **25** (2016) 1630005.
[34] ALICE Collaboration, CERN-ALICE-PUBLIC-2017-001.
[35] J. L. Albacete *et al.*, arXiv:1707.09973 [hep-ph].